L-Subshell Resolved Photon Angular Distribution of Radiative Electron Capture into He-like Uranium

Th. Stöhlker,[1] H. Geissel,[1] H. Irnich,[1] T. Kandler,[1] C. Kozhuharov,[1] P. H. Mokler,[1] G. Münzenberg,[1] F. Nickel,[1] C. Scheidenberger,[1] T. Suzuki,[1] M. Kucharski,[2] A. Warczak,[2] P. Rymuza,[3] Z. Stachura,[4] A. Kriessbach,[5] D. Dauvergne,[6] B. Dunford,[7] J. Eichler,[8] A. Ichihara,[9] and T. Shirai[9]

[1]*Gesellschaft für Schwerionenforschung (GSI), Planckstr. 1, 64291 Darmstadt, Germany*
[2]*Jagiellonian University, Institute of Physics, 30-059 Cracow, Poland*
[3]*Institute for Nuclear Studies, 05-400 Swierk, Poland*
[4]*Institute of Nuclear Physics, 31-342 Cracow, Poland*
[5]*Institut für Kernphysik der Universität Frankfurt, 60486 Frankfurt, Germany*
[6]*Institut de Physique Nucléaire, Université Lyon I, 69622 Villeurbanne Cedex, France*
[7]*Physics Division, Argonne National Laboratory, Argonne, Illinois 60439*
[8]*Bereich Theoretische Physik, Hahn-Meitner-Institut Berlin, 14109 Berlin, Germany*
[9]*Japan Atomic Energy Research Institute, Tokai-mura, Ibaraki 319-11, Japan*

(Received 3 June 1994)

The photon angular distributions for radiative electron capture (REC) into the $j = 1/2$ and $j = 3/2$ L subshell levels were measured and calculated for $U^{90+} \rightarrow C$ collisions at 89 MeV/u. The experiment provides the first study of the photon angular distribution of REC into a projectile p state ($j = 3/2$) which was found to exhibit a slight backward peaking in the laboratory frame. For radiative capture to the $j = 1/2$ states, the measured angular distribution deviates considerably from symmetry around 90°. The results demonstrate that the usual $\sin^2\theta_{lab}$ distribution is not valid in the high-Z regime.

PACS numbers: 31.30.Jv, 34.70.+e

In collisions of highly charged ions with free or quasifree electrons, the projectile may capture an electron into a bound state. If this process is accompanied by the simultaneous emission of a photon, it is denoted as "radiative electron capture" (REC). Experimental studies during the last years [1–3] have mainly focused on REC to the K shell of light and medium-Z projectiles, while results for higher shells are rather scarce [2,4]. In this Letter, we report the first dedicated experimental and theoretical study of the strongly anisotropic photon-angular distribution for REC into the energy-resolved substates of the L shell of a high-Z projectile. The subshell-dependent photon-angular distributions probe details of the relativistic bound-state wave functions and, at forward (or backward) angles, the contribution of the electron spin caused by magnetic interaction in relativistic collisions [5,6]. There is no other case, up to now, in which spin-flip effects in relativistic atomic collisions can be studied so directly. We also note that detailed information on REC is of essential importance for accelerator-based atomic structure studies of high-Z ions, where this process is the most important production mechanism for excited projectile states [4,7].

Until now, the only measurement of x-ray angular distributions in REC has been reported by Anholt *et al.* [8] for capture into the K shell of bare 197 MeV/u Xe ions from Be atoms. In this case, the prediction of the nonrelativistic treatment [9] was approximately verified. If one adopts a dipole approximation for the electron photon interaction for capture into an s state [10], the angular distribution of the emitted photon in the projectile system is proportional to $\sin^2\theta$ where θ is the angle between the incoming electron and the emitted photon. However, if retardation effects are included, the radiation pattern is bent into the backward direction and, only after transforming into the laboratory frame, one ends up with a $\sin^2\theta_{lab}$ distribution, as has been first noted by Spindler, Betz, and Bell [11] and confirmed experimentally in [8]. Very recently, Ichihara, Shirai, and Eichler [6] performed relativistic calculations using exact bound and continuum wave functions and treating the accurate electron momentum distribution in the low-Z target atoms within the impulse approximation. For high-Z projectiles, they predicted pronounced deviations from a $\sin^2\theta_{lab}$ distribution for K-shell as well as for L-shell REC. For the latter, the results can be tested only in measurements of subshell resolved angular distributions. This is done and theoretically analyzed in the present Letter.

The experimental study of the photon angular distribution for REC into the substates of the L shell reported here was performed at the fragment separator (FRS) at GSI Darmstadt [12]. He-like uranium ions were chosen as projectiles which can be produced with sufficient intensity even at an energy as low as 89 MeV/u. Due to the moderate Doppler broadening at this collision velocity of $\beta = 0.41$ ($\beta = v/c$) and the large L-subshell splitting between the $j = 1/2$ and $j = 3/2$ states of about 4 keV rendered possible for the first time to separate REC into the different j substates of the L shell. It allows an exploratory study of the photon angular distribution for REC into a pure p state ($j = 3/2$). For our experimental investigation, the $2s(j = 1/2)$ and the $2p(j = 1/2)$ levels

 0031-9007/94/73(26)/3520(4)$06.00

in Li-like uranium, which are separated only by about 280 eV, can be treated as approximately degenerate.

For the experiment, the charge state fraction of the He-like ion species was magnetically separated at the first two stages of the FRS and focused onto a 400 $\mu g/cm^2$ thick carbon reaction target with a diameter of 3 cm, mounted at the central focal plane at the FRS. The target itself was tilted with respect to the ion optical axis by 30°. After penetrating the reaction target, the emerging charge states were once more magnetically analyzed in the two final stages of the FRS and directed onto scintillator detectors mounted at the final focal plane. Here, the ions with the primary charge state (90+) and the ions which captured one electron (89+) in the reaction target could be registered independently in fast scintillator particle counters.

For detection of projectile x rays, the target area was surrounded by five solid-state Ge(i) detectors viewing the target chamber center at observation angles of 30°, 45°, 90°, 135°, and 150° with respect to the beam axis. We have to emphasize that the simultaneous measurement at the various observation angles enabled us to determine precisely the relative x-ray yields of the detectors independently of the primary beam intensity. The solid angle of each detector amounted to $\Delta\Omega/4\pi \sim 10^{-3}$. At 45°, 90°, and 135°, conventional x-ray detectors were installed with crystals of the thickness of 20, 15, and 12 mm and active areas of 800, 200, and 250 mm^2, respectively. At 45° and 135° these areas were defined by rectangular slits mounted just in front of the detectors. At 30° and 150°, 15 mm thick, specially designed granular detectors were used [7], consisting of seven equidistant, parallel stripes allowing to cover observation angles between $27° \leq \theta_{lab} \leq 33°$ and $146° \leq \theta_{lab} \leq 154°$, respectively. The x rays registered by each detector (detector segment) were recorded event by event in coincidence with the down-charged ions.

In Fig. 1 the L-REC spectra are shown, taken at the observation angles of 45°, 90°, and 135° in coincidence with projectiles having captured one electron. Although the

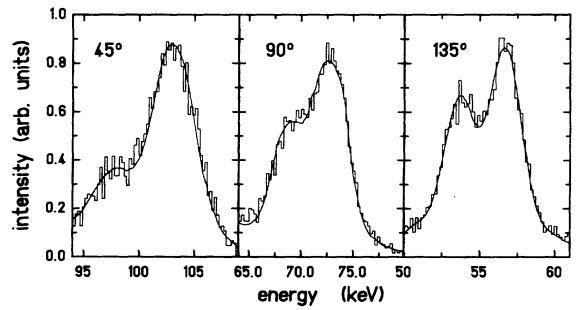

FIG. 1. Charge-state-coincident L-REC spectra measured under different observation angles in the laboratory frame for 89 MeV/u $U^{90+} \rightarrow C$ collisions. For presentation, the intensities were normalized to one common scale. The solid lines are fitted calculations (see text).

L-REC line shape is smeared out by the Compton profile of the carbon target electrons, the splitting of the spectral distribution, due to the L-subshell splitting, is clearly visible. The most remarkable feature of the spectra is the very strong variation of the relative intensities of the components ($j = 3/2$ and $j = 1/2$, see the low- and the high-energy part of the spectra in the figure, respectively) with respect to the observation angle.

In order to gain precisely the line intensities corresponding to REC into the $j = 1/2$ and $j = 3/2$ states, the L-REC spectra were fitted for each angle using a theoretical line shape based on the double differential cross section [13] which incorporates the correct Compton profiles of the target electrons [14]. The results were transformed to the laboratory frame and convoluted by a rectangular function in order to account for the Doppler broadening. In addition, a linear background was considered. In order to improve the statistical significance of the analysis, the spectra of the sevenfold detector at 150° were summed up to three data sets at slightly different centroid angles. The appropriate choice of the applied spectral line shape analysis is demonstrated in Fig. 1 by the solid lines. For the evaluation of the differential cross sections, the line yields for each j substate gained by the least squares fit were solid-angle corrected and normalized to the primary beam intensity. For the latter, a total normalization uncertainty of 50% must be assumed, whereas the relative systematic uncertainties of the differential cross section values for the various angles can be estimated to be less than 6%. In Fig. 2, the obtained differential cross section values are given as a function of the observation angle [see full diamonds in Fig. 2(a) for capture to the $j = 1/2$ states and in Fig. 2(b) for capture to the $j = 3/2$ level]. The data are compared with theoretical predictions based on a rigorous treatment of the REC process [6], which uses (a) exact relativistic Coulomb wave functions for the bound and continuum projectile states, (b) accurate Hartree-Fock momentum distributions of the electrons in their initial target states, and (c) rigorous addition of the initial electron momenta with the momentum resulting from the translation motion of the target with respect to the projectile. In the case considered here, the Li-like U^{89+} is replaced by a hydrogenic system with the effective charge $Z_{eff} = 90.3$ [see full lines in Figs. 2(a) and 2(b)]. In Fig. 2(a) the predicted angular distributions for REC into the $2s_{1/2}$ state (dashed curve) and into the $2p_{1/2}$ state (dotted line) are given separately. All measured data points were multiplied by one common factor of 0.65 for the adjustment to the theoretical predictions, which is still within the total absolute uncertainty of the measurement. As seen in Figs. 2(a) and 2(b), a good agreement between experiment and theory can be stated. The data for the $j = 1/2$ levels deviate considerably from a symmetry around 90°, whereas the radiation pattern for REC into the $2p_{3/2}$ state shows a slight enhancement at backward angles. As illustrated in Fig. 2(a), the forward peaking for REC into the $j = 1/2$ sublevels can be

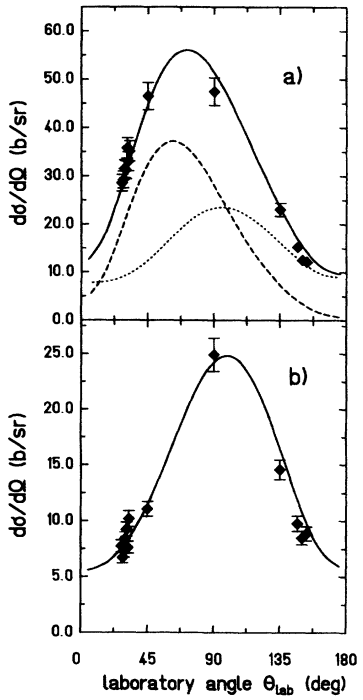

FIG. 2. Experimental angular distribution of L-REC radiation (diamonds) for (a) REC into the $2s_{1/2}$ and $2p_{1/2}$ states and (b) REC into the $2p_{3/2}$ level. The solid line shows the result derived from relativistic exact calculations. Theoretical results for capture into the $2s_{1/2}$ state [dashed line in (a)] and for capture into the $2p_{1/2}$ state [dotted line in (a)] are shown separately.

explained by transitions to the $2s_{1/2}$ state [compare dashed line in Fig. 2(a)]. Following Ichihara, Shirai, and Eichler [6], this forward shift is partially attributed to the occurrence of spin-flip transitions (magnetic transitions). In the case of REC to the $2s_{1/2}$ state, only magnetic transitions can produce nonvanishing cross sections at the forward ($\theta_{lab} = 0°$) or the backward ($\theta_{lab} = 180°$) angle. In contrast to the forward direction, the distribution at backward angles is essentially determined by radiative transitions to the $2p_{1/2}$ state [compare dotted line in Fig. 2(a)]. This radiation pattern is very similar to the one seen in Fig. 2(b) for capture into the $2p_{3/2}$ state where the Lorentz transformation is not quite sufficient to cancel the backward shift caused by retardation.

The striking difference of the two measured angular distributions becomes more pronounced if the ratio of REC into $j = 3/2$ and $j = 1/2$ levels is presented as a function of the observation angle (Fig. 3). The results of the relativistic calculation are given by the full line in Fig. 3, whereas the experimental data are represented by full points. The measured ratio is not affected by possible systematic uncertainties, and the error bars shown are essentially due to the statistical uncertainty. The predicted very pronounced forward-backward asymmetry is excellently reproduced by the experiment. The ratio reaches its minimum at an observation angle of 45°, whereas the maximum occurs at a backward angle of about 150°. Between minimum and maximum the intensity ratio changes by as much as a factor of 2.6.

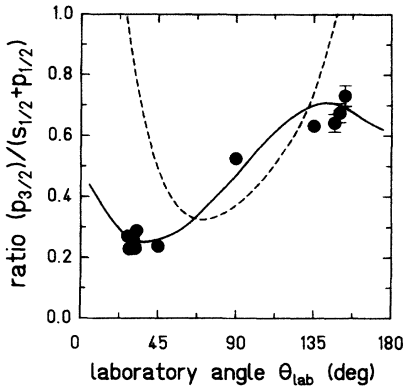

FIG. 3. Measured intensity ratios (see full points) as a function of the observation angle in comparison with theoretical predictions (solid line, relativistic-exact calculation; dashed line, nonrelativistic approximation including lowest-order retardation effects [15]).

We like to add that the agreement found in Fig. 3 implies strongly that the predicted total subshell population cross sections are also correct. These values are given in Table I in comparison to the results of the nonrelativistic approximation. This comparison manifests that the population of the two p states does not follow a pure statistical distribution, one of the basic assumptions of a nonrelativistic approach. The nonrelativistic dipole approximation underestimates the capture to the $2p$ states by about 40% (compare Table I). However, for REC to the $2s$ state, the result is very close to the relativistic one. A similar observation for K-REC (capture to the $1s$ state) has already been reported by Stöhlker *et al.* [2]. For completeness, the predictions of the nonrelativistic approach including lowest-order retardation effects are also illustrated in Fig. 3 (compare dashed line) [15]. As seen in the figure, this approach fails completely in describing the measured data.

TABLE I. Comparison of L-subshell population cross sections (given in barn) calulated within the relativistic theory (RT) [6] and the dipole approximation (DA) [10,15] using an effective projectile charge of 90.3. For the relativistic calculations, convergence was obtained by including all partial waves with the relativistic quantum number $|\kappa| \leq 10$.

	$\sigma_{2s_{1/2}}$	$\sigma_{2p_{1/2}}$	$\sigma_{2p_{3/2}}$
RT	274.6	219.7	219.7
DA	261.6	89.7	179.5

In conclusion, the subshell resolved REC measurement elucidates the subtleties of the radiative electron capture process. The results are in excellent agreement with exact relativistic calculations and show pronounced deviations from a $\sin^2\theta_{lab}$ distribution. Nonvanishing cross sections in the forward and backward directions point to the importance of magnetic transitions for REC into high-Z projectiles. In addition, the relevance of the angular momentum of the final state wave function is manifested by the observed intensity pattern for REC into the $2p_{3/2}$ state. We conclude that proper relativistic calculations must be used for reliable subshell cross section predictions which are of crucial importance for planned atomic structure studies using high-Z ions. For example, on the basis of our findings, the discrepancy between the relative intensities for K-, L-, and higher-shell REC as discussed by Beyer *et al.* [4] is expected to be removed if a proper relativistic theory is applied.

In the near future it is planned to extend our investigations to highly relativistic as well as to slow bare heavy ions. For the latter, the deceleration mode of the ESR storage ring will be used, allowing to decelerate high-Z ions up to bare uranium to energies below 20 MeV/u. The angular differential information at such low beam energies will provide an important tool for the correct understanding of x-ray spectra taken from high-Z ions at the cooler section of storage rings, especially when measured solely under one specific angle. Note that at such low velocities one is essentially sensitive to the relativistic character of the final state wave function. Complementary to the low energy regime, the use of highly relativistic heavy ions will provide additional information on spin-flip transitions which are extremely sensitive to the use of accurate wave functions.

The work of three of us, M. K., Z. S., and A. W., was supported by GSI in Darmstadt and by the State Committee for Scientific Research (Poland) under Research Grant No. 201779101.

[1] H. Tawara, P. Richard, and K. Kawatsura, Phys. Rev. A **26**, 154 (1982).
[2] Th. Stöhlker *et al.*, Z. Phys. D **23**, 121 (1992).
[3] C. R. Vane *et al.*, Phys. Rev. A **49**, 1487 (1994).
[4] H. F. Beyer *et al.*, J. Phys. B **26**, 1557 (1993).
[5] J. Eichler, Phys. Rep. **193**, 165 (1990).
[6] A. Ichihara, T. Shirai, and J. Eichler, Phys. Rev. A **49**, 1875 (1994).
[7] Th. Stöhlker *et al.*, Phys. Rev. Lett. **71**, 2184 (1993).
[8] R. Anholt *et al.*, Phys. Rev. Lett. **53**, 234 (1984).
[9] H. A. Bethe and E. E. Salpeter, *Quantum Mechanics of One- and Two- Electron Atoms* (Springer-Verlag, Berlin, 1957).
[10] M. Stobbe, Ann. Phys. (Paris) **7**, 661 (1930).
[11] E. Spindler, H.-D. Betz, and F. Bell, Phys. Rev. Lett. **42**, 832 (1979).
[12] H. Geissel *et al.*, Nucl. Instrum. Methods Phys. Res., Sect. B **70**, 286 (1992).
[13] M. Kleber and D. H. Jakubassa, Nucl. Phys. **A252**, 152 (1974).
[14] F. Biggs, L. B. Mendelsohn, and J. B. Mann, At. Data Nucl. Data Tables **16**, 201 (1975).
[15] K. Hino and T. Watanabe, Phys. Rev. A **36**, 5862 (1987).